Hand-eye-calibration of a robotized thermography end-effector

Thomas SCHMIDT,
German Aerospace Center, Institute of Structures and Design, Center for Lightweight-Production-Technology (ZLP), Am Technologiezentrum 4, 86159 Augsburg, Germany
Phone: +49-821-319874-1050; Mobile: +49-172-8343570; Fax: +49-8153-281028,
E-mail: t.schmidt@dlr.de

Abstract. The application of active thermography applied as Lock-in or pulse thermography has been widely used in aerospace industry. Over the last years a number of activities had been undertaken to achieve a higher level of automation. Industrial robots are very versatile and allow a comparably easy integration of a measurement system in robotic workcell further the control unit. It is therefore possible to cover a large range of geometrical complex parts even on larger dimensions. The robot can be used for the positioning of the thermography camera and delivers the location of the robot flange coordinate system at the time of measurement automatically. It is then necessary to know the offset between flange coordinate system and camera coordinate system.
The approach at DLR Augsburg of a robot based measuring system for industrial thermography applications has been presented in previous papers. With this paper DLR-Center for Lightweight-Production-Technology in Augsburg will give insight into current work in the area of hand-eye-calibration of a robotized thermography end-effector and results derived from first experiments.

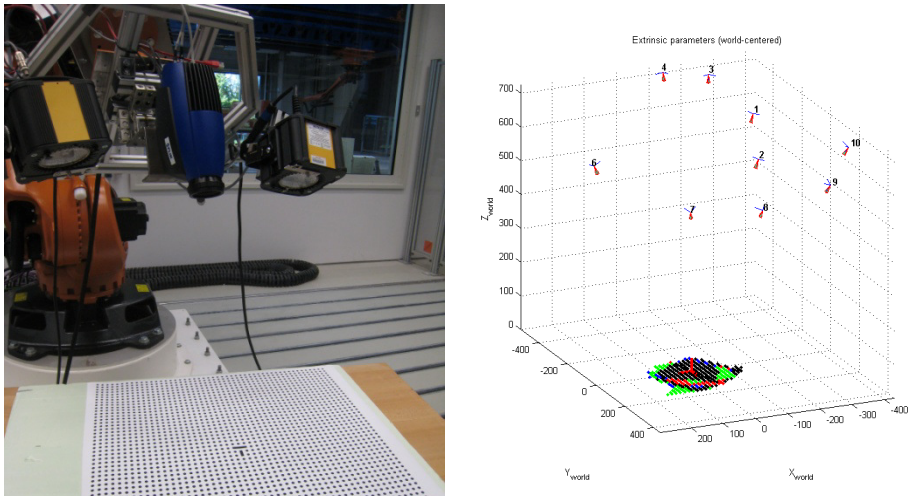

Figure 1 hand-eye-calibration of a robotized thermography end-effector

Keywords: automated lock-in thermography, hand-eye calibration, robotized end-effector, infrared camera

1 Introduction

Earlier studies have demonstrated the effectivity of lock-in thermography as an ideal measure to perform contactless and thus non-destructive testing along the manufacturing process chain of composite material. At DLR a system had been developed that enables automated lock-in thermography even for large scale structures. The system consists of modular components which are the following:

1. Standard Lock-in thermography device with adaptable automation interface
2. Industrial robot as a manipulator
3. Programmable controller with interchangeable memory as a link in between the both mentioned above

The actual concept had been presented in previous papers [1] and [2]. Here, insight will be given into one of the challenges that arise when a camera is mounted on an end-effector for an industrial robot in order to create a highly flexible but accurate measurement system.

1.1 Prototype of robotic end-effector

In previous papers the concept of the robotic end-effector had been presented [1]. So to keep this short just the fundamental features will be highlighted. The end-effector consists of a standard flange that connects towards the robotic hand. The load carrying structure itself had been built from aluminum profiles. The profiles can be adjusted in length and their position can be changed, the end-effector is therefore able to carry up to 3 halogen lamps in a very flexible constellation. Additionally the elevation of the camera can be adjusted. Figure 2 shows some examples of the end-effector.

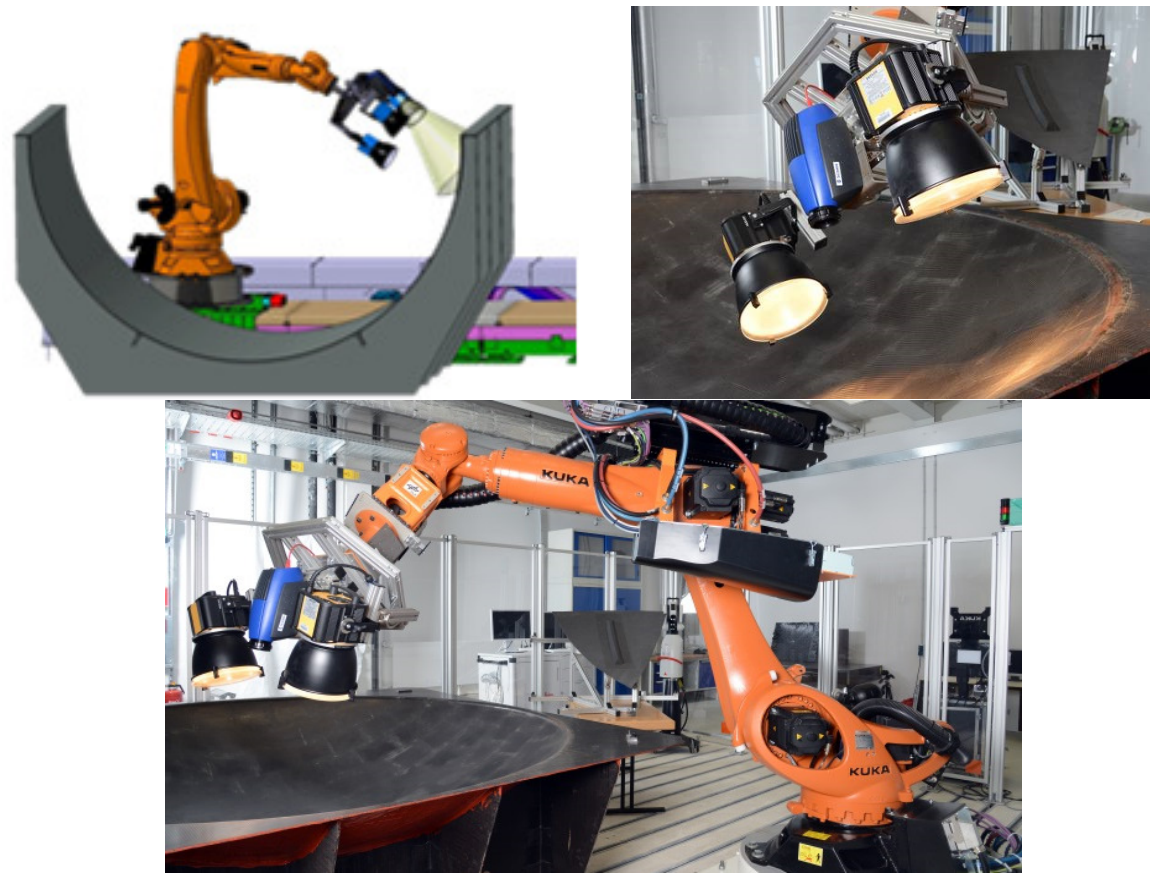

Figure 2 Robotic end-effector mounted on industrial robot

1.2 Description of main challenge

With all the adjustability of your camera one achieves a high flexibility on the one hand, but challenges on the other hand as well. In order to relate measurements made by a sensor mounted on a mechanical link to the robot's coordinate frame we must first estimate the transformation between the sensor and the link frame. Figure 3 shows the current situation the flange coordinate system so called NullFrame is known through the kinematic chain of the robot and the tool center point (TCP) is of interest.
It is possible to get an estimation of your installation by using CAD data, but usually inaccuracies in your assembly or the absence of knowledge about your optical system makes it impossible to predict this relationship.

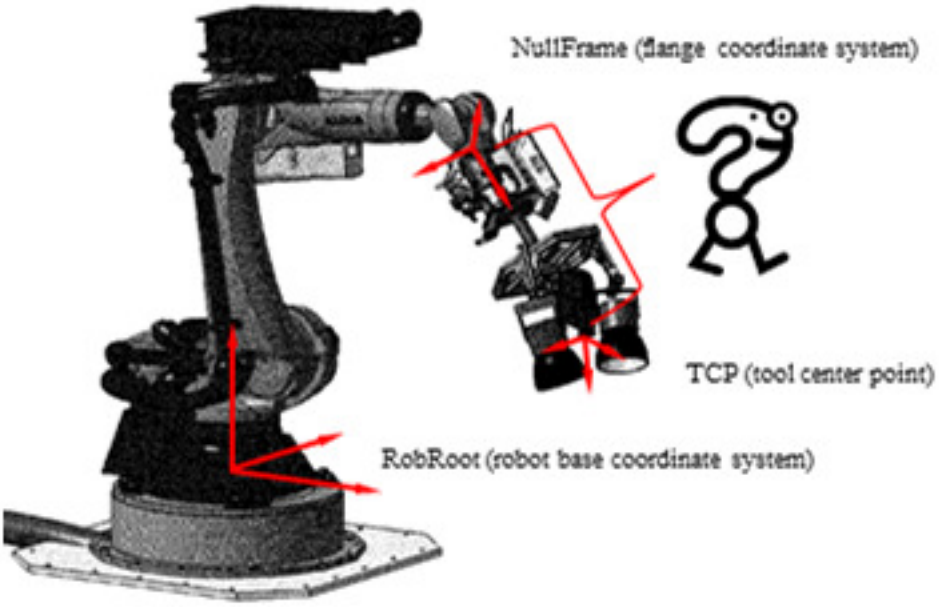

Figure 3 principal question of a sensor mounted on a robot

A possible solution for this problem is called hand-eye calibration which stands for the computation of the relative position and orientation between the robot flange and a camera mounted rigidly on the flange. The problem concerns also all sensors that are rigidly mounted on mechanical links, like a camera mounted on a binocular head with mechanical degrees of freedom as well as a camera mounted on a vehicle. Although the term sensor-actuator calibration is more appropriate the author will throughout this paper use the well known term "hand-eye".
A common approach is to use the camera itself in order to get the offset values from flange coordinate system to camera coordinate system. Feuerstein [3] gives a great overview on several approaches. A literature study brought up that the Bougetj implementation [4] in combination with the work from ETH Zurich [5] were the most appropriate in our case.

1.3 Hand-eye calibration procedure in a nutshell

The procedure requires a minimum of 10 images taken from a pattern as shown below (Figure 4). The robot acting as a manipulator moves the camera to various locations. Each time the position and orientation of the robot flange is stored. Both, the images as well as the position and orientation of Nullframe, are fed into the given toolbox. The toolbox then analyses the images, performs pattern recognition, does a calibration of the images and calculates the offset values from camera coordinates to flange coordinate system as well as other optical parameters.

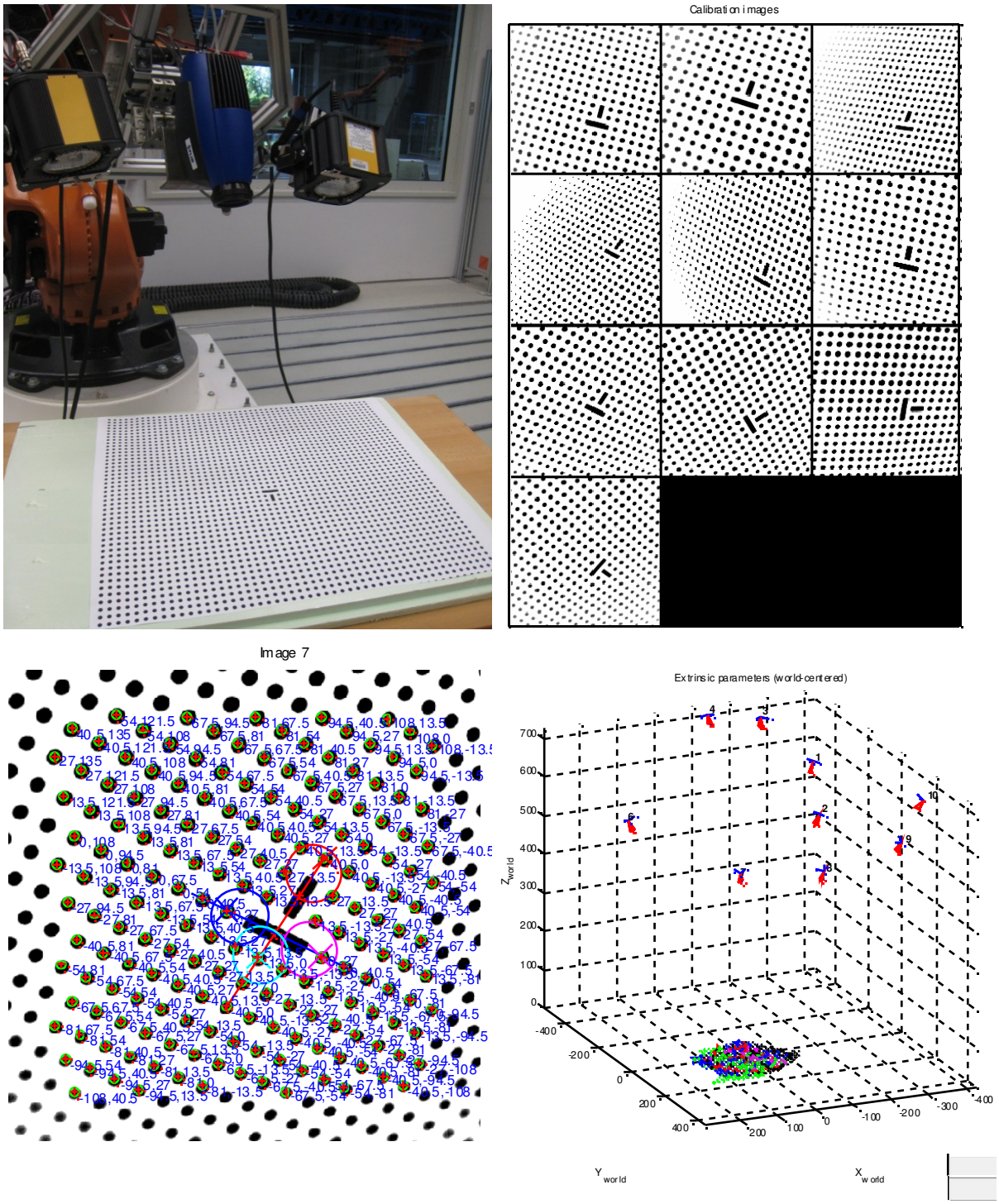

Figure 4 Hand Eye Calibration Procedure (top left – robot with thermography camera mounted on end-effector, top right – calibration images, bottom left – processed calibration image example, bottom right – hand eye calibration results in world view)

1.4 How to get good images?

As described under 1.3 it is mandatory to have a number of 10 images available in order to perform proper hand-eye calibration. The problem now occurs that an infrared camera produces images at room temperature that are very blurry as long as there are no temperature gradients, shown in Figure 5.

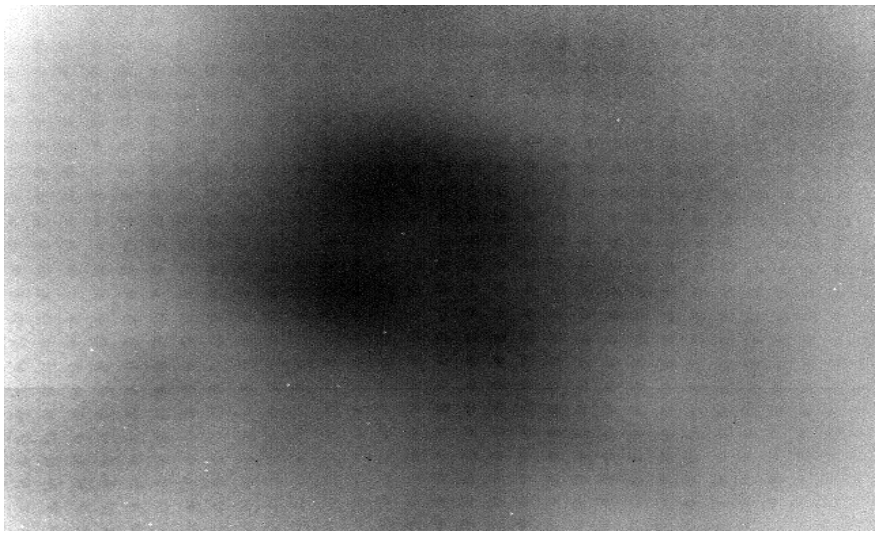

Figure 5 Image from dotted pattern taken from infrared camera at room temperature

To overcome this issue active thermography, optically excited lock-in thermography in particularly, had been used. Best results by using the inverted amplitude image had been achieved as depicted in Figure 6.

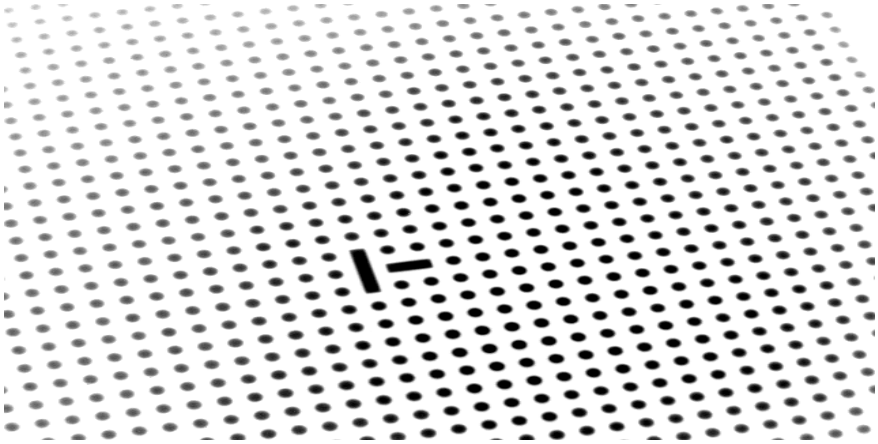

Figure 6 Inverted amplitude image taken from lock-in thermography

First trials had been undertaken by using a printed black and white pattern on cardboard produced with a commercial plotter. The results didn't show satisfying accuracy in particular the thermal stability of the test pattern was inadequate as well as the fact that the cardboard showed humidity uptake and therefore strong distortions. Best results had been achieved by using a thermal stable material, the pattern had been printed with a professional printing machine of higher accuracy.

2 Iterative approach

The used camera has an autofocus function and no fixed lens which is very helpful in most applications. When using the robot as a manipulator it is possible to keep the distance between camera and object constant but if necessary the distance might be changed. Nevertheless after each change of focal length hand-eye calibration needs to be performed. The information than can be stored. Best practise showed that an iterative approach worked quite well. In a first step the robot had been taught to 10 positions where the distance between camera and pattern had been close to constant. Performing a hand-eye calibration

delivered a Pre-TCP. In a second step this Pre-TCP had been used in an offline programming environment as tool data, see Figure 7. Again a number of 10 points, this time with a constant distance to the pattern, had been defined. Subsequently the hand-eye calibration had been repeated until the desired accuracy had been achieved.

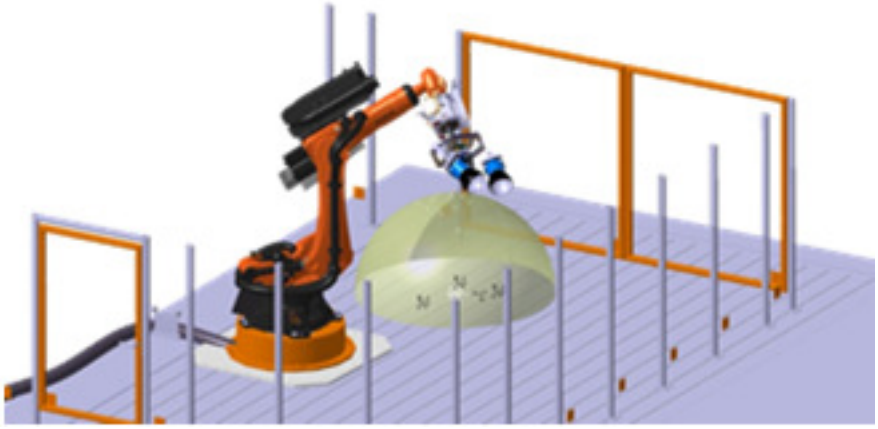

Figure 7 Using offline programming for collision free determination of measurement points

After a first iteration the so called reprojection error had been investigated as shown in Figure 8. It shows already satisfactory results of ±0.25px in X and ±0.25px in Y (red circle). Points outside this region are outliers and are a result of an inhomogeneous excitation during lock-in thermography.

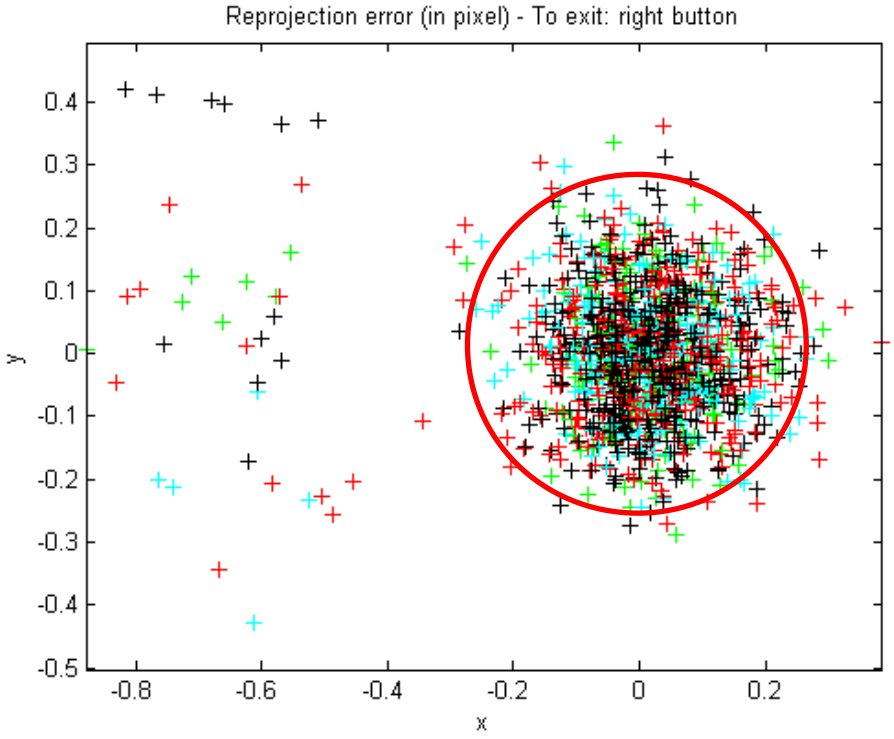

Figure 8 Reprojection error after hand-eye calibration

Using the reprojection information allows to recalculate the skew and distortion of the optical system of the camera. For a better visibility of this issue the image below had been chosen. Figure 9 shows the strongly distorted image due to an inappropriate pattern material. The results showed clearly the occurrence of local deformations of the pattern.

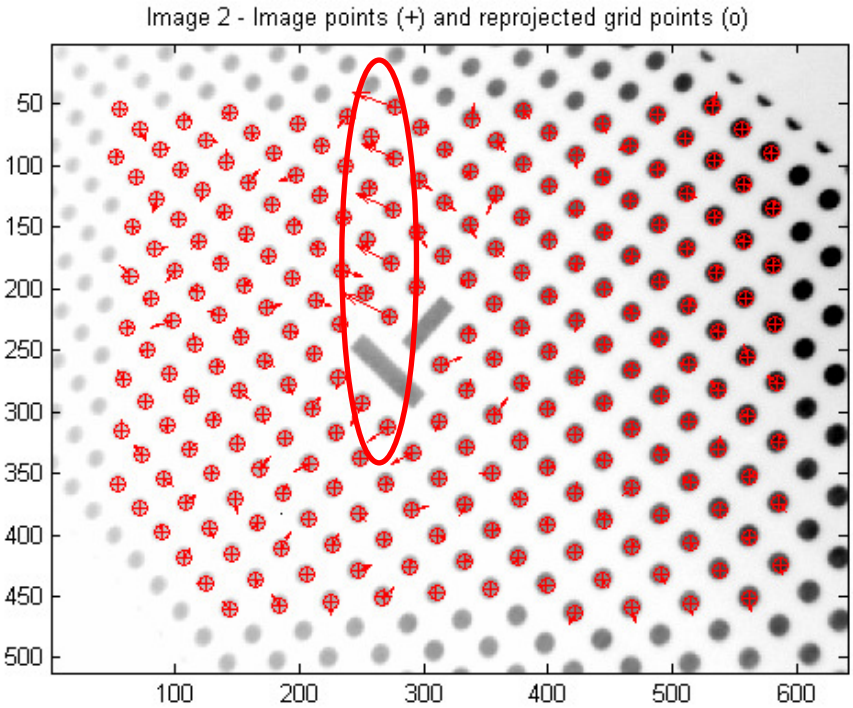

Figure 9 Example for local distortions as an effect of inappropriate pattern material

Finally this procedure can also be used to correct the thermography images from the optical effects by using the camera matrix and the distortion matrix [6].

3 Results from experiments

The results can be subdivided into two sets of information:

1. Camera related results
2. Hand-eye related results

and can be summarized as followed:

3.1 Camera related results

The used toolbox delivers values for focal length (current setup), principal point, distortion coefficients as well as the pixel error. Skew had been disregarded so far.

All calibration results (with uncertainties) as given below:

Table 1 Camera calibration results

Focal Length:	fc =	[1973.20306 1969.91104] ± [3.55756 3.31701] mm
Principal point:	cc =	[293.88650 255.12651] ± [5.91518 4.43811] px
Skew:	alpha_c =	not been optimized yet
Distortion:	kc =	[-0.43104 0.96768 -0.00047 0.00047 0.00000] ± [0.03405 1.10513 0.00040 0.00035 0.00000]
Pixel error:	err =	[0.14661 0.10570] px

The focal length comes with an uncertainty of less than 0,2% which is a satisfactory result. The principal point is not in the middle of the camera system (Image size 640 x 512px) as expected but undergoes quite extreme deviations. Reasons for this are not yet discovered,

further studies need to be done. Values for the focal length and the principal point will feed the so called camera matrix.
The distortion coefficients take radial and tangential factors into account. The presence of the radial distortion manifests in form of the "barrel" or "fish-eye" effect. Tangential distortion occurs because the image taking lenses are not perfectly parallel to the imaging plane. Both components, radial (k_1, k_2, k_3) and tangential (p_1, p_2), are calculated according to [6] and can be presented in a one row matrix with 5 columns, the so called distortion matrix.

$$\boldsymbol{Distortion_{coefficients}} = (\boldsymbol{k_1\ k_2\ p_1\ p_2\ k_3}) \quad \text{.....(1)}$$

The largest deviations can be found within the radial distortion components. This results from disadvantageous pattern material in combination with uneven excitation during the measurement of the images. The pixel error, also called reprojection error, had been achieved after suppressing 3 of the 10 images with very large outliers.

3.2 Hand-eye related results

Performing the experiments gives back homogenous transformation matrices of such form:

$$H_{cam2flange} = \begin{bmatrix} & R_{cam2flange} & & T_{cam2flange} \\ 0 & 0 & 0 & 1 \end{bmatrix} \quad \text{.....(2)}$$

For example one measurement results in values according to Table 2.

Table 2 Hand-eye example results (rotatory comp. in light grey, translational comp. in dark grey)

-0,8715	-0,2394	-0,4279	-123,0687
0,4902	-0,4056	-0,7715	-201,0337
0,0111	-0,8822	0,4708	952,8292
0	0	0	1

The experiments had been performed six times under same conditions; results are given in Table 3. For a better understanding and to achieve input values for the robot control unit the values from each transformation matrices (e.g. Table 2) had been reverse calculated to a notation in X, Y, Z, A, B, C as presented in Table 3.

Table 3 Results from hand eye calibration

Average Translation [mm]		Standard Deviation [mm]	Average Rotation [°]		Standard Deviation [°]
X	-123,0427	0,281	A	150,643	0,012
Y	-201,0124	0,163	B	-0,635	0,086
Z	952,6491	0,507	C	-61,912	0,046

The results given in Table 3 represent the tool center point (TCP) which had later been used for other work. The deviations are relatively small and derive from the repetitive accuracy of the industrial robot which is comparably good. The reason for this can be found in the use of a high accuracy robot. The effect of absolute accuracy had not been investigated yet.

Current work is concerned about a validation scenario for the values above which independent from this method.

4 Conclusions

Within this study DLR has successfully demonstrated the feasibility of hand-eye calibration for a robotized thermography end-effector. The presented results give now confidence in the localization of the measured image. This allows localizing occurrences in the parts investigated, even on large parts e.g. 10 x 20 m, by using an industrial robot as a manipulator in combination of such end-effector in order to achieve adequate accuracy. There is still room for improvement as it was mentioned the image acquisition can be improved, the accuracy of the pattern plays a key role, finally the lock-in parameters need a fine tuning for each pattern. Further work needs to be done with a wider spectrum of "working distances" resp. focal lengths of the camera to generate broader knowledge for further applications. The camera and distortion matrix will be used in the future to undistort the thermography images for a geometrically accurate representation of occurrences or defects.

Acknowledgements
This work had been founded by the state government of Bavaria, the city of Augsburg and DLR and the initial funding of the start-up project of the Center for Lightweight-Production-Technology (ZLP). Special thanks go to team members of ZLP Augsburg, namely Alfons Schuster, Manfred Schönheits and Christian Nissler for their contributions and support.

References

[1] T. Schmidt, "Automation in Production Integrated NDT Using Thermography," in *NDT in Aerospace*, Augsburg, 2012.

[2] T. Schmidt, "CFRP manufacturing process chain observation by means of automated thermography," in *NDT in Aerospace*, Singapore, 2013.

[3] M. Feuerstein, "Hand-Eye Calibration," Technical University of Munich, [Online]. Available: http://campar.in.tum.de/Chair/HandEyeCalibration. [Accessed 08 2013].

[4] J.-Y. Bouguetj, "Camera Calibration Toolbox for Matlab," [Online]. Available: http://www.vision.caltech.edu/bouguetj/calib_doc/. [Accessed 10 2013].

[5] E. Zurich, "Fully automatic camera and hand to eye calibration," [Online]. Available: https://www.vision.ee.ethz.ch/software/calibration_toolbox/calibration_toolbox.php. [Accessed 10 2013].

[6] o. d. team, "OpenCV 2.4.9.0 documentation," 2014. [Online]. Available: http://docs.opencv.org/doc/tutorials/calib3d/camera_calibration/camera_calibration.html. [Accessed July 2014].